Analysis of belt transmissions capabilities using the brush model

F Bucchi* and F Frendo

Department of Civil and Industrial Engineering, University of Pisa - Largo Lucio Lazzarino, 56122 - Pisa, Italy

E-mail: *francesco.bucchi@unipi.it, francesco.frendo@unipi.it

Abstract.

The mechanics of power transmission is usually modeled by two different theories: the creep theory and the shear theory. Recently, the authors introduced an alternative theory based on the brush model, which allows to compute the tangential stress distribution along the winding arc of pulleys. The brush model is able to predict the speed loss along the driving and driven pulley as a function of the transmission parameters (e.g. pre-load, friction, pulley radii etc.) and the operating parameters (i.e. angular speed and resistant torque). In addition, the energy efficiency of the system is obtained by knowing the speed loss and the energy dissipation; this contribution can be subdivided into energy loss due to friction and energy loss due to the non-recoverable elastic deformation of the bristle.

In the present paper, using the previously developed model, a sensitivity analysis aimed at mapping the transmission capabilities as a function of geometry and operating parameters is proposed. These results, given as look-up table (or contour plot), are very important in mechanical systems simulation (e.g. real-time systems, hardware in the loop systems) since they allow to introduce the phenomenological behavior of the pulley-belt transmission without introducing complex models in the simulation.

1. Introduction

Power transmission is a key-topic in mechanical engineering and pulley-belt transmissions are widely used in many industrial applications. The mechanics of belt transmissions have been studied for centuries and several models were proposed to describe the transmission capability and the transmission efficiency. During XVIII century Euler was the first to link the tension of a rope along a pulley to the friction between the rope/belt and the pulley. Later, the speed losses caused by belt deformation where considered by Reynolds in 1875 and the effect of the centrifugal force was implemented by Grashof in 1883. More recently many papers extended the Grashof model, often called creep model, including the effects of inertia, bending stiffness, different belt cross section etc. All these models divide the winding arc along the pulleys in two regions: the adhesion region and the sliding region. In the adhesion region, it is assumed that the tangential stress between the belt and the pulley is zero and the belt tension does not vary. On the other hand, micro-slip or creep occurs along the sliding region, due to tangential stresses related to friction between belt and pulley. Alternatively to the creep model, Firbank in 1970 proposed a model assuming that the angular deformation (shear) of the belt causes the belt tension variation along the adhesion arc. This deformation is due to the tangential speed difference between belt and pulley. Even if some hypotheses on the shear deformation are introduced, the *Firbank* model does not compute the angular coordinate where slip begins considering friction limits, but divides the adhesion and slip regions

in order to satisfy the belt tension values at the entrance and at the exit of the pulley. The *Firbank* model has also been extended in order to consider extensible belts [1].

In the paper [2] the authors introduced a new mechanical model, inspired to the "brush model" used in the description of the mechanical behavior of pneumatic tires [3]–[5], which can describe, in steady–state conditions, the trend, along the contact arc, of the belt tension and the tangential stress between belt and pulley. The detailed knowledge of the contact actions provides an estimate of the power losses related to the contact between belt and pulleys and to the elastic deformation of the belt (see e.g. [4]). The model considers the transition between static and dynamic friction based on Coulomb friction model and faces with the *stick–slip* phenomenon which may occur along the winding arc. Indeed, Della Pietra and Timpone in [6] measured the belt tension by means of strain gauges bonded on the belt surface and observed the *stick–slip* phenomenon. Stick and slip is also mentioned in [7], where the normal and tangential forces acting on the pulleys are measured by force transducers for the case of an abrasive belt. In the literature, this phenomenon is considered also in papers studying the sliding of the rubber and is investigated in [8]–[9]. In addition, in [10] the authors extended the "brush model" to extensible belts by introducing the continuity equations and discussed the effect of the belt elasticity on the main operating parameters of a given transmission.

In the present paper, using the previously developed models, a sensitivity analysis aimed at mapping the transmission capabilities as a function of geometry and operating parameters is proposed. Transmission capability maps are presented showing the driven pulley speed and the transmission efficiency as a function of driving pulley speed and resistant torque for different belt pre-loads, friction coefficients, pulley radii, belt axial stiffness etc. These results, given as look-up table (or contour plot), are very important in mechanical systems simulation (e.g. real-time systems, hardware in the loop systems) since they allow to introduce the phenomenological behavior of the pulley-belt transmission without introducing complex models in the simulation. In addition, the results are also useful during the design phase of a transmission since they allow to select and, eventually, optimize the set of parameters, which determine the transmission kinematics and efficiency.

2. Mathematical model of the belt transmission

The mathematical model implemented to perform the sensitivity analysis is the one developed in [10] which is recalled in this section.

The belt is assumed as composed of the tension member, made of the reinforcement fibers which are much stiffer than the rubber matrix, composed of a bed of elastically deformable bristles in contact with the pulley. The model is planar and the following equations are valid per unit of width of the belt. Figure 1 shows a schematic of the problem where the main geometry, static and kinematic parameters are given: R_{dg} and R_{dn} are the driving and the driven pulleys' radii, ω_{dg} and ω_{dn} is the driving and driven pulley angular velocity and M_{dg} and M_{dn} are the torques acting on the driving and driven pulley, respectively.

Considering the continuity equation, for a given angular coordinate α, the belt velocity V_{b} and the belt tension T are linked by the following relationship

$$V_{\mathrm{b}}(\alpha) = v_1 \frac{EA + T(\alpha)}{EA + T_1} = v_2 \frac{EA + T(\alpha)}{EA + T_2} \tag{1}$$

where T_1 and T_2 are the belt tension on the tight and slack side, respectively, EA represents the longitudinal stiffness per unit width of the belt, v_1 [v_2] is the peripheral speed of the belt in correspondence of the belt tension T_1 [T_2].

The bristles transmit a tangential stress τ to the pulley which is assumed proportional to the bristle deformation s

$$\tau = k_{\mathrm{s}}\, s \tag{2}$$

being k_{s} the bristle stiffness.

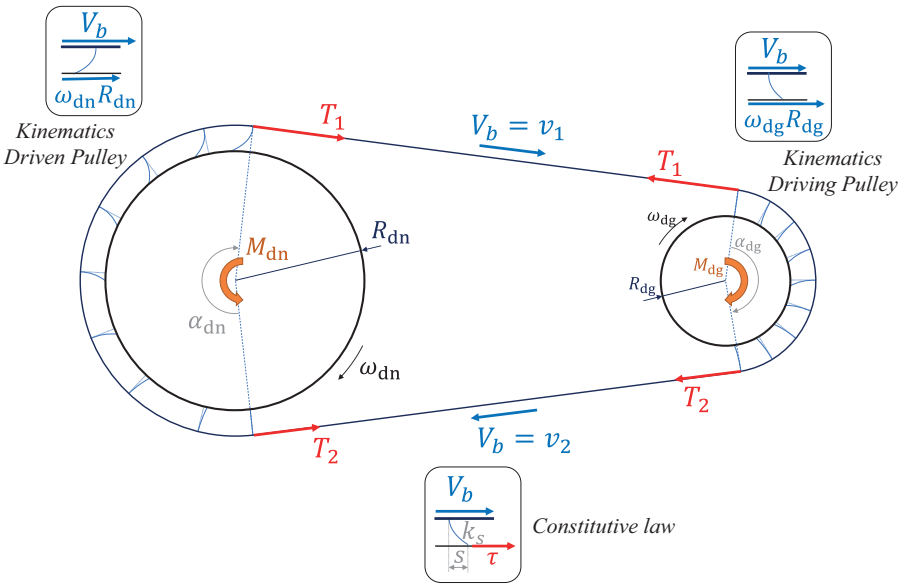

Figure 1. Belt transmission schematic and brush model concept.

When a bristle enters into the pulley, the difference of speed between the tension member and the peripheral speed of the pulley causes the bristle deformations and tangential stress due to friction between the belt and the pulley. The static friction occurs until the adhesion limit condition is reached

$$\tau \leq \tau_s = \mu_s \, p \tag{3}$$

where μ_s is the static friction coefficient and p is the normal pressure, which is given by the well known relationship

$$p = \frac{T - q V_b^2}{R} \tag{4}$$

with q the lineic mass of the belt.

Figures 2–3 shows a qualitative representation of the contact stress and the friction limit along the driving pulley (left) and driven (right) pulley. As demonstrated analytically in [2] and [10], the contact stress rises with the angular coordinate along both the driving and driven pulleys, up it reaches the friction limit. Once the static friction limit has been reached, stick–slip can occur.

The tangential stress τ reaches the static friction limit τ_s in correspondence of the angular coordinates called $\alpha^{(i)}_{s,dg}$ (along the driving pulley) and $\alpha^{(i)}_{s,dn}$ (along the driven pulley). The index i counts the number of occurrences for which the friction limit has been reached.

For each angular section included between two friction limit occurrences ($\alpha^{(i)}_{s,dg} < \alpha < \alpha^{(i+1)}_{s,dg}$) along the driving pulley, the belt tension expression is obtained [10] in closed–form as follows:

$$\begin{aligned} T^{(i+1)}_{dg}(\alpha) = & \frac{-M + \left(M + N\, T^{(i)}(\alpha_{s,dg})\right) \cosh\left(\sqrt{N}\left(\alpha - \alpha^{(i)}_{s,dg}\right)\right)}{N} \\ & - \frac{\mu_d \, p(\alpha^{(i)}_{s,dg}) \, R_{dg} \sinh\left(\sqrt{N}\left(\alpha - \alpha^{(i)}_{s,dg}\right)\right)}{\sqrt{N}} \end{aligned} \tag{5}$$

where

$$M = -k_s \, R^2_{dg} + k_s \, v_1 \frac{R_{dg}}{\omega_{dg}} \frac{EA}{EA + T_1} \tag{6}$$

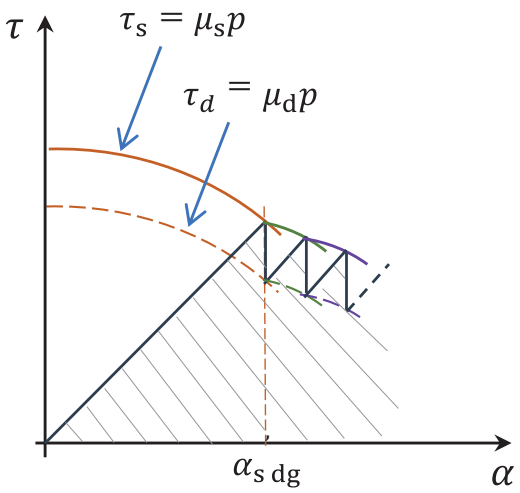

Figure 2. Representation of the contact stress and the friction limit: Driving pulley.

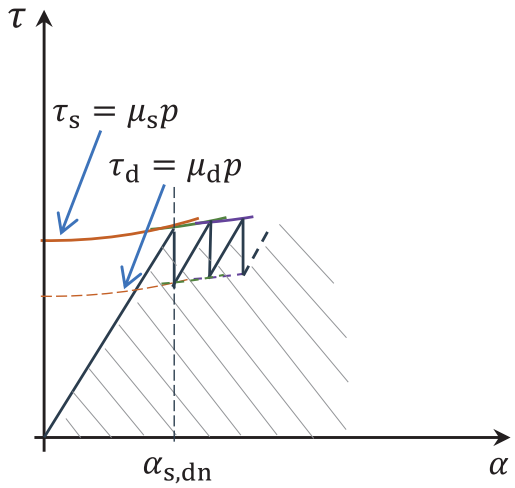

Figure 3. Representation of the contact stress and the friction limit: Driven pulley.

and

$$N = \frac{k_s\, v_1 R_{\mathrm{dg}}}{\omega_{\mathrm{dg}}(EA + T_1)} \tag{7}$$

Similarly, for $\alpha_{\mathrm{s,dn}}^{(i)} < \alpha < \alpha_{\mathrm{s,dn}}^{(i+1)}$ along the driven pulley, the belt tension is

$$T_{\mathrm{dn}}^{(i+1)}(\alpha) = \frac{-P + \left(P + Q\, T^{(i)}(\alpha_{\mathrm{s,dn}})\right) \cosh\left(\sqrt{Q}\left(\alpha - \alpha_{\mathrm{s,dn}}^{(i)}\right)\right)}{Q} + \frac{\mu_d\, p(\alpha_{\mathrm{s,dn}}^{(i)})\, R_{\mathrm{dn}} \sinh\left(\sqrt{Q}\left(\alpha - \alpha_{\mathrm{s,dg}}^{(i)}\right)\right)}{\sqrt{Q}} \tag{8}$$

with

$$P = -k_s\, R_{\mathrm{dn}}^2 + k_s\, v_2 \frac{R_{\mathrm{dn}}}{\omega_{\mathrm{dn}}} \frac{EA}{EA + T_2} \tag{9}$$

and

$$Q = \frac{k_s\, v_2\, R_{\mathrm{dn}}}{\omega_{\mathrm{dn}}(EA + T_2)} \tag{10}$$

3. Model implementation

The brush-model was implemented in the Mathematica© basing on the scheme shown in figure 4. Using this model it is possible to obtain information about the transmission capability (e.g. transmissible moment) and the efficiency of the belt-pulley system as a function of the input parameters.

The resistant torque M_{dn} applied to the driven pulley, the angular velocity ω_{dg} of the driving pulley, the belt pre–load T_0 and the pulley radii, R_{dg} and R_{dn} are given as input parameters, along with the belt pre–load T_0; by solving the set of governing equations, the tensions on the tight and slack side of the belt are determined.

The goal of the routine is to compute v_1 and ω_{dn} and to this aim two *while*-loops have been implemented. The first while loop, assuming a first attempt velocity $v_1^{(1)}$ computes the belt tension at the

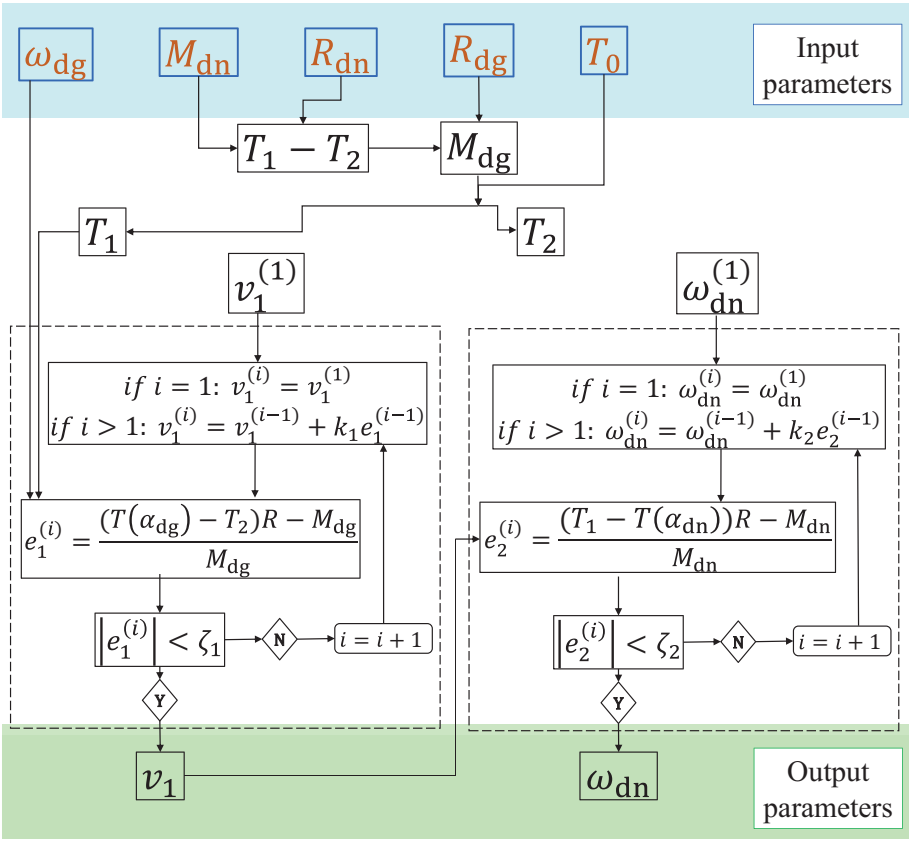

Figure 4. Schematic of the flow chart explaining the model implementation.

exit from the driving pulley $T(\alpha_{dg})$ and compares it to the belt slack side tension T_2. The error $e_1^{(i)}$ is computed and it is used to correct the belt entering velocity, until the error is lower than the threshold ζ_1.

Known v_1, in a similar way the second *while*-loop computes the driven pulley angular velocity ω_{dn}.

4. Energy efficiency computation

In this model the dissipated energy is divided in energy dissipated due to contact slip (friction) and non-recoverable potential energy due to the deformation of the bristles exiting from the pulleys. The transmission efficiency is the ratio between power transmitted by the driven and driving pulley respectively, as follows

$$\eta = \frac{M_{dn}\omega_{dn}}{M_{dg}\omega_{dg}} \tag{11}$$

In particular, as already done in [2], let D_{dg} and D_{dn} indicate the energy dissipated by friction, for the driving and driven pulley, respectively:

$$D_{dg} = \sum_{i=1}^{N_{dg}} T(\alpha_{dg}^i)(s_{dg}^i(\alpha_{dg}^i) - s_{dg}^{i+1}(\alpha_{dg}^i)) \tag{12}$$

$$D_{dn} = \sum_{i=1}^{N_{dn}} T(\alpha_{dn}^i)(s_{dn}^i(\alpha_{dn}^i) - s_{dn}^{i+1}(\alpha_{dn}^i)) \tag{13}$$

where α^i_{dg} and α^i_{dn} are the angle on the driving or driven pulley where the friction limit is reached for the $i-$th time, $s^i_{\text{s,dg}}$ and $s^i_{\text{s,dn}}$ represent the bristle slip which takes place at angular position α^i_{dg} and α^i_{dn} and N_{dg} and N_{dn} represents the total number of slip events. The terms U_{dg} and U_{dn} are the elastic potential energy stored in the bristle:

$$U_{\text{dg}} = \frac{1}{2} k_s \, s^2_{\text{dg}}(\pi) \, \pi \, R_{\text{dg}} \tag{14}$$

$$U_{\text{dn}} = \frac{1}{2} k_s \, s^2_{\text{dn}}(\pi) \, \pi \, R_{\text{dn}} \tag{15}$$

where $s_{\text{dg}}(\pi)$ and $s_{\text{dn}}(\pi)$ is the elastic deformation of the bristle exiting from the driving and driven pulley, respectively.

5. Sensitivity analysis

In order to to test the model and to assess the transmission capability of a belt-pulley transmission, several sensitivity analyses have been performed varying separately: the belt pre–load, the friction coefficient, the angular velocity of the driven pulley and the belt stiffness. The reference parameters considered for the model are those given in previous work [2] and [10] by the authors and summarized in table 1.

Table 1. Model parameters.

Symbol	Parameter	Units	Value
R_{dg}	Driving pulley radius	mm	40
R_{dn}	Driven pulley radius	mm	40
ω_{dg}	Driving pulley angular velocity	rad/s	300
k_{s}	Bristle stiffness	N/m^2	5.072 $\times 10^6$
μ_{d}	Dynamic friction coefficient	-	0.3
μ_{s}	Static friction coefficient	-	0.36
q	Belt mass per unit length	kg/m	0.24
T_0	Belt pre–load	N	400
EA	Belt stiffness	N	inf

5.1. Effect of the pre–load

The belt pre–load has been varied in the range 300–500 N and the results in terms of driven pulley velocity as a function of transmitted torque are shown in figure 5.

The results refers to the condition for which dynamic friction has been reached on both the driving and driven pulleys. The extrapolation of the results in the region where static friction occurs along, at least, one entire pulley is shown through dashed lines. For a given pre–load, as the torque rises, the driven pulley velocity decreases up to an almost-vertical asymptote which represents the dynamic (stick–slip) friction along the whole pulleys' winding arc. As the pre–load rises the transmissible torque rises and the velocity loss, for a given value of transmitted torque, is lower. It is worth noting that, since the pulley radii are the same, the driving and driven torque are the same and, consequently, the velocity loss are directly related to the efficiency of the transmission: indeed the efficiency is the ration between the driven pulley angular velocity and the driving pulley angular velocity.

Figures 6–9 shows the energy dissipated due to friction along the driving and driven pulley, D_{dg} and D_{dn} respectively, and the energy loss due to elastic potential energy stored in the bristle for the driving and driven pulley, U_{dg} and U_{dn} respectively. These are refereed to an angular rotation of the driving pulley of 180°.

For a given pre–load the energy dissipated due to friction along both the driving and driven pulleys rises as the transmitted torque rises, while the effect of the pre–load is similar to a translation in the

horizontal direction of the plot. The energy dissipated due to potential energy stored in the bristles at the exit of the pulley slightly varies for a given pre–load and clearly increases as the pre–load rises. For the driving pulley, except for very low values of transmitted torque, the energy dissipated due to friction is much higher than the energy dissipated due to elastic energy stored at the exit of the pulley, which is negligible. This is due to the fact that the bristle deformation at the exit of the pulley is low due to the low value of the normal pressure. Globally, for a given working condition, the energy dissipated along the driving pulley is higher than the energy dissipated along the driven pulley, mainly because the sliding (stick–slip) arc along the driving pulley is larger.

5.2. Effect of the friction coefficient

Similarly to the belt pre–load, the friction coefficient between pulleys and belt has been varied in the range 0.2–0.3 and the results in terms of driven pulley velocity as a function of transmitted torque are shown in figure 10. The effect of the friction coefficient is very similar to the effect of the belt pre–load: as the friction coefficient increases, the transmitted torque increases. Similar considerations to the one already expressed in the pre–load section can be drawn also about the dissipated energy, whose trends are shown in figures 11–14.

5.3. Effect of the driving pulley angular velocity

Figure 15 show the normalized velocity ($\bar{\omega}_{dn} = \omega_{dn}/\omega_{dg}$) of the driven pulley as a function of the transmitted torque for different angular velocities of the driving pulley.

The effects, both in terms of angular velocity and in terms of dissipated energy (figures 16–19), are qualitatively comparable to the ones already discussed for the pre–load and friction coefficient variations. In particular, as the angular speed of the driving pulley rises the transmissible torque reduces and the velocity loss, for a given value of transmitted torque, rises. This effect is similar to a reduction of the friction coefficient (or of the effective pre–load) and it is due to the centrifugal force which increases following a quadratic law as the angular speed increases, producing a reduction of the normal pressure between belt and pulley and consequently a reduction of the transmissible torque capability.

In order to support this hypothesis, a sensitivity analysis has been performed for different driving pulley angular velocities computed without considering the lineic mass of the belt, excluding in this way the effect of the centrifugal force. The results are shown in figure 20 and figures 21–24. As expected, the results are overlapped for all the driving pulley angular velocities.

5.4. Effect of the belt elasticity

Finally, a sensitivity analysis was performed varying the belt stiffness per unit of width EA (where E is the equivalent belt elasticity and A the cross-section area of the belt) in the range 50-700 kN. Figure 25 shows the driven pulley angular velocity as a function of the transmitted torque and figures 26–29 shows the energy dissipated. In the considered stiffness range the effect of the elasticity is not pronounced and some differences can be found only for very low value of stiffness (i.e. 50 or 100 kN), while for stiffer belts the results are almost overlapped to the infinitely stiff belt. Where appreciable, the reduction of the belt stiffness causes a slightly higher velocity loss for low transmitted torque (i.e. about 11 Nm) and slightly higher energy dissipated due to friction; this effect can be ascribed to the fact that, as discussed in [10], for lower values of belt stiffness the stick-slip zone is larger. On the contrary, for higher values of transmitted torque the effect of the belt elasticity is not appreciable.

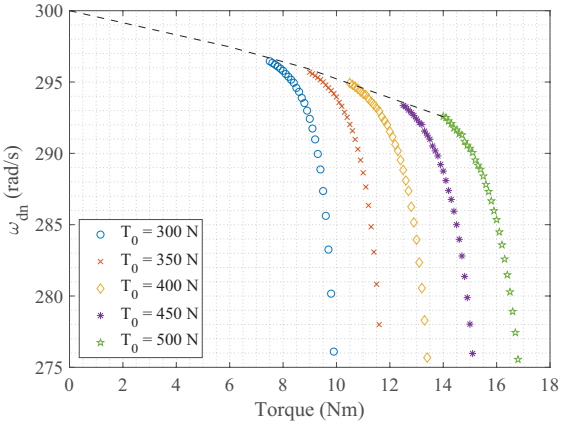

Figure 5. Driven pulley velocity for different pre–loads.

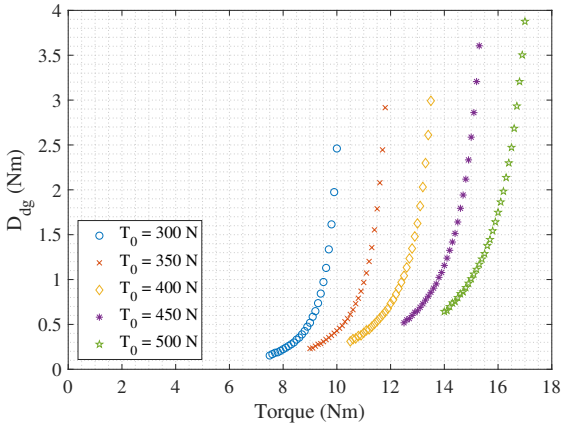

Figure 6. Friction energy dissipated along for different pre–loads - Driving pulley.

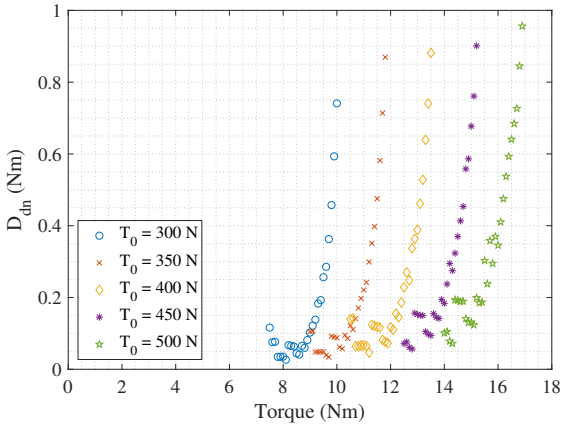

Figure 7. Friction energy dissipated for different pre–loads - Driven pulley.

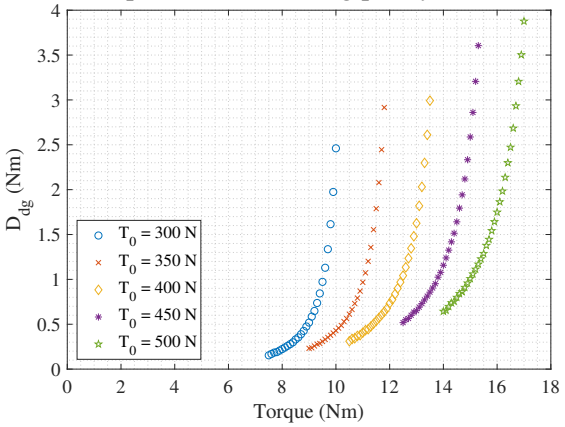

Figure 8. Potential energy stored in the belt for different pre–loads - Driving pulley.

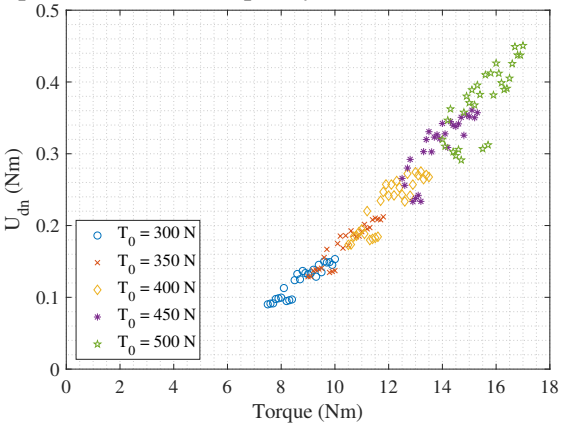

Figure 9. Potential energy stored in the belt exiting for different pre–loads - Driven Pulley.

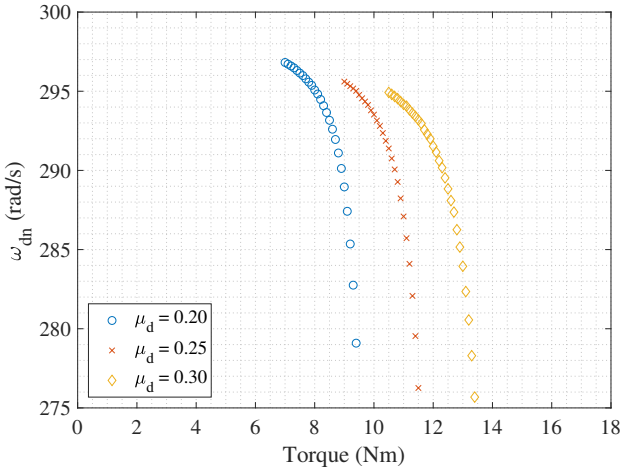

Figure 10. Driven pulley velocity for different friction coefficients.

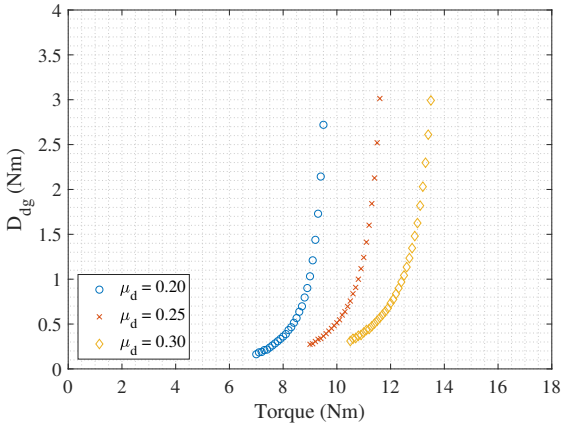

Figure 11. Friction energy dissipated for different friction coefficients - Driving pulley.

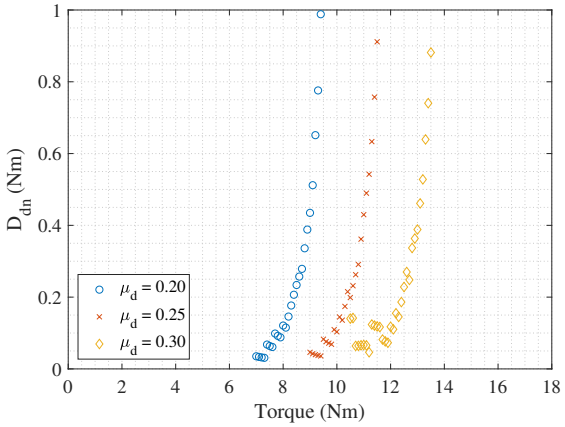

Figure 12. Friction energy dissipated for different friction coefficients - Driven pulley.

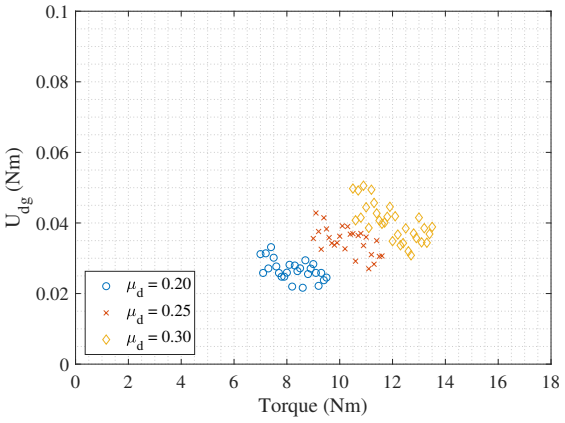

Figure 13. Potential energy stored in the belt for different friction coefficients - Driving pulley.

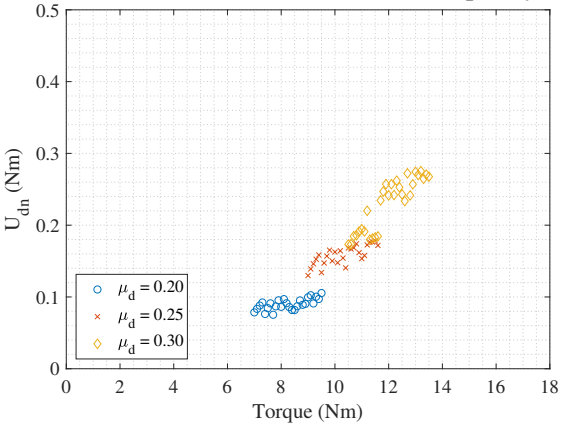

Figure 14. Potential energy stored in the belt for different friction coefficients - Driven pulley.

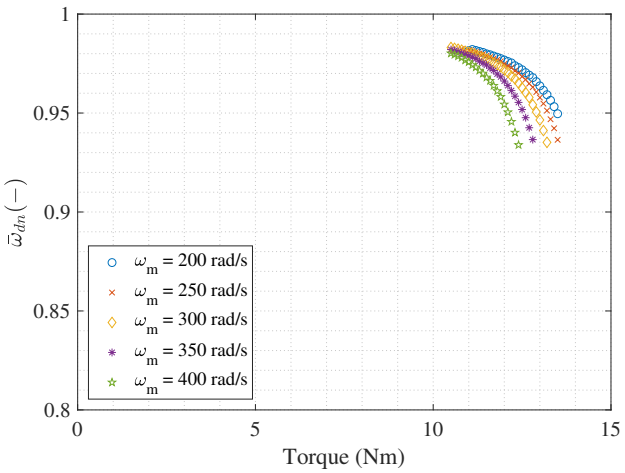

Figure 15. Normalized driven pulley velocity for different driving pulley angular velocities.

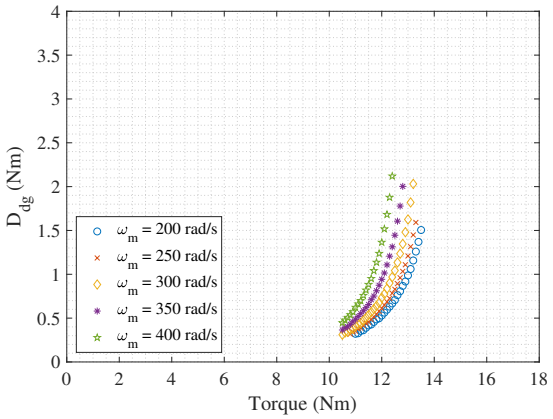

Figure 16. Friction energy dissipated for different driving pulley angular velocities - Driving pulley.

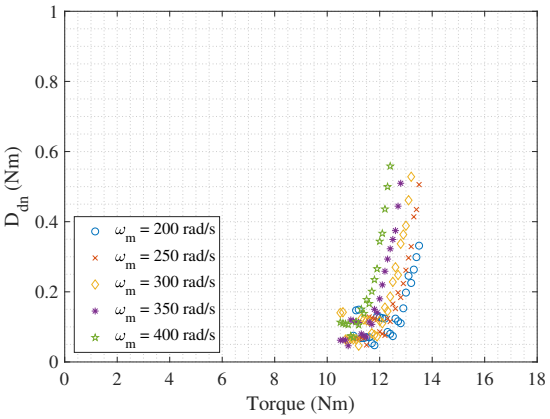

Figure 17. Friction energy dissipated for different driving pulley angular velocities - Driven pulley.

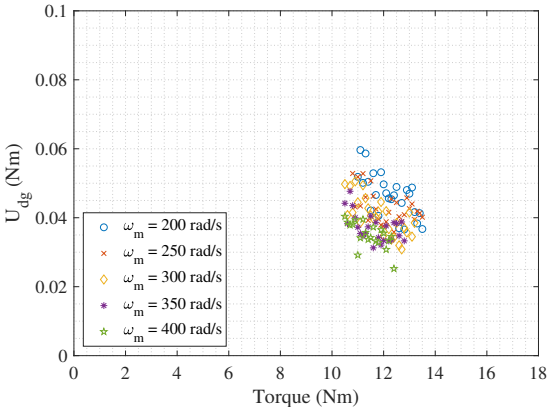

Figure 18. Potential energy stored in the belt for different driving pulley angular velocities - Driving pulley.

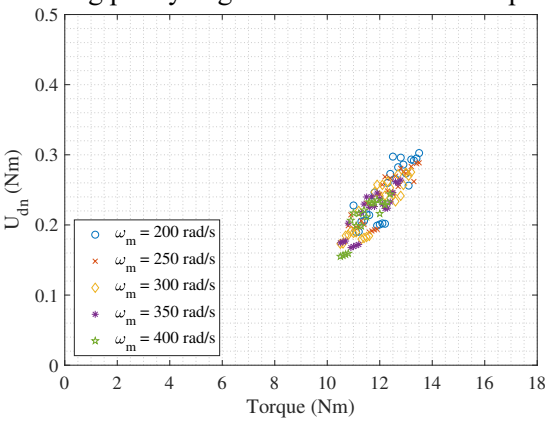

Figure 19. Potential energy stored in the belt for different driving pulley angular velocities - Driven pulley.

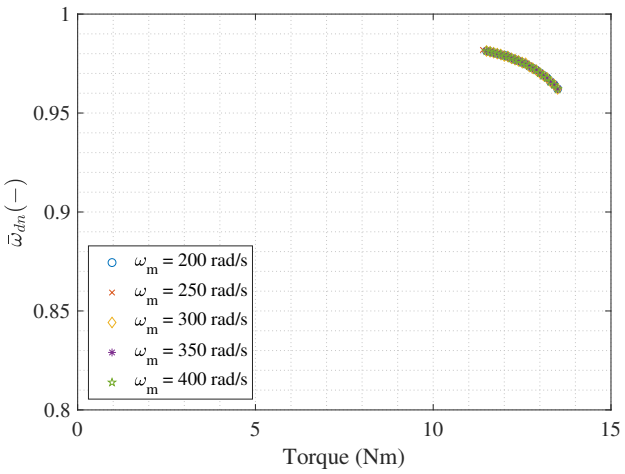

Figure 20. Normalized driven pulley velocity for different angular velocities - No centrifugal force.

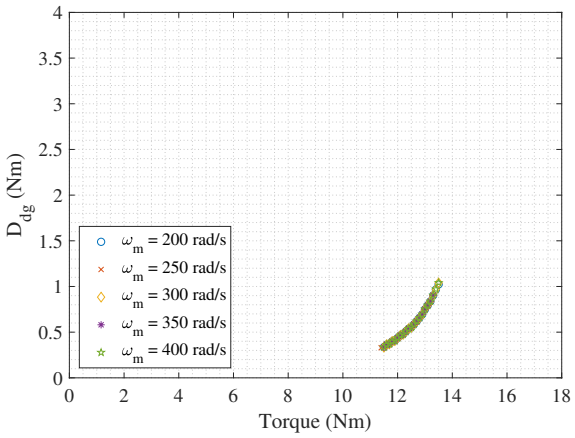

Figure 21. Friction energy dissipated for different driving pulley angular velocities - No centrifugal force - Driving pulley.

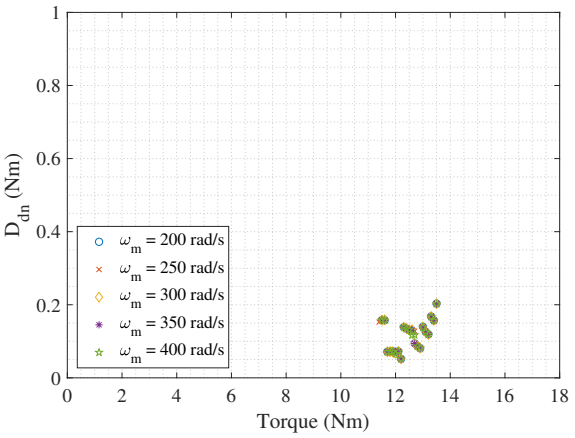

Figure 22. Friction energy dissipated for different driving pulley angular velocities - No centrifugal force - Driven pulley.

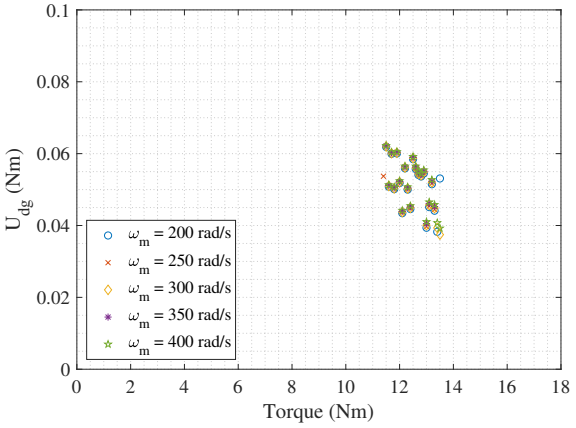

Figure 23. Potential energy stored in the belt for different driving pulley angular velocities - No centrifugal force - Driving pulley.

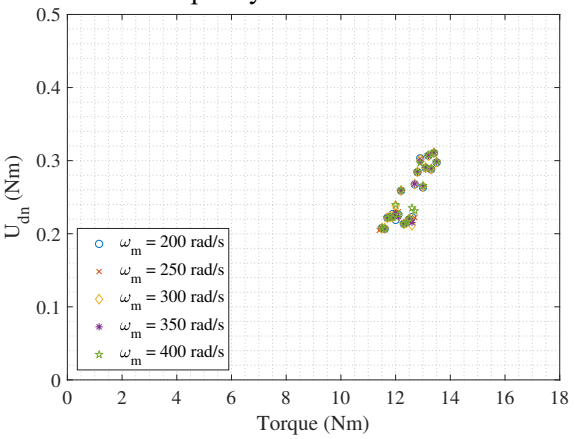

Figure 24. Potential energy stored in the belt for different driving pulley angular velocities - No centrifugal force - Driven pulley.

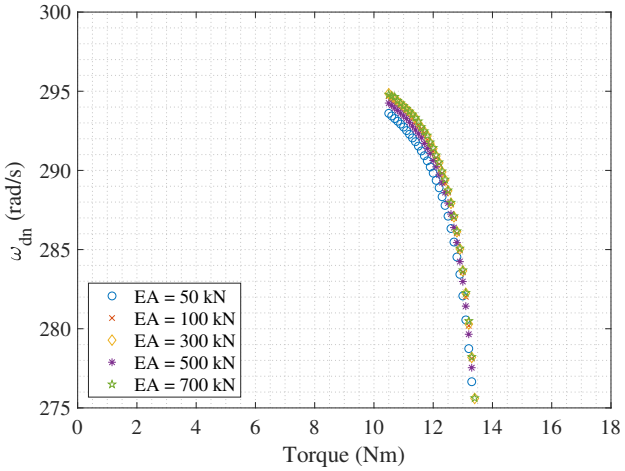

Figure 25. Normalized driven pulley velocity as a function of transmitted torque for different belt stiffnesses.

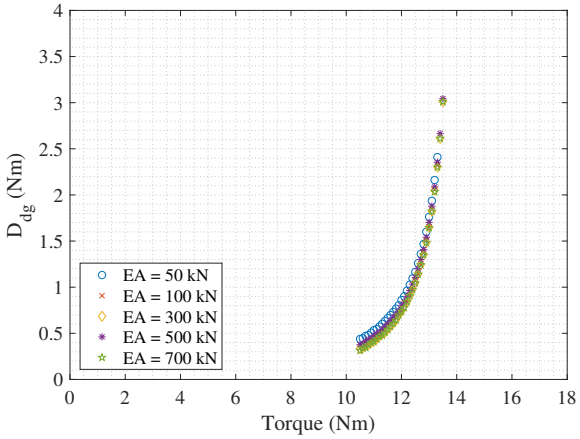

Figure 26. Friction energy dissipated along the driving pulley for different belt stiffnesses.

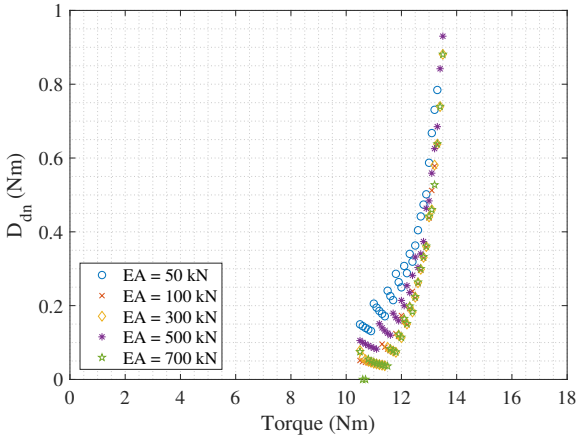

Figure 27. Friction energy dissipated along the driven pulley for different belt stiffnesses.

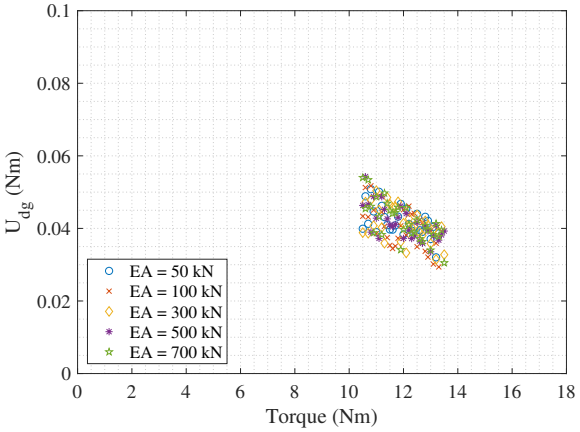

Figure 28. Potential energy stored in the belt exiting from the driving pulley for different different belt stiffnesses.

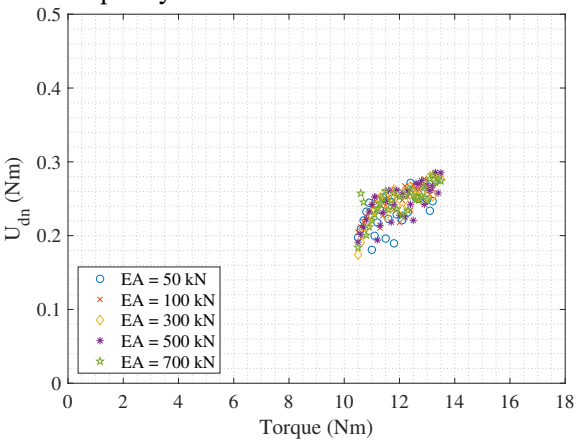

Figure 29. Potential energy stored in the belt exiting from the driven pulley for different belt stiffnesses.

6. Conclusions

In this paper a numerical sensitivity analysis of the transmission capability of a pulley-belt transmission has been performed. The analysis considered steady-state operation of flat belts and it has been performed using a model previously developed by the authors, based on ”brush” model, frequently used to model pneumatic tire behavior. The simulations were performed imposing the angular velocity at the driving pulley and the resistant torque at the driven pulley. The model allowed to compute the belt and the driven pulley velocity and the dissipated energy.

The pre–load, the friction coefficient, the angular velocity of the driving pulley and the belt stiffness have been varied, one at a time, in order to infer their effect on the transmission capability of the pulley-belt system. As predictable, increasing the pre–load and the friction coefficient allows to transmit higher values of torque and, for a given value of torque, to dissipate a lower amount of energy. Concerning the angular velocity of the driving pulley, if it is increased the effect is opposite to the pre–load or friction coefficient increase, because higher angular velocity causes higher velocity of the belt and, consequently, higher values of centrifugal force, which reduces the effective tension of the belt and the normal pressure between the belt and the pulley, negatively affecting the transmission capability. It is interesting to point out that if the centrifugal force is neglected, assuming very low value of the lineic mass of the belt, the effect of the variation of the driving pulley angular velocity is negligible in the analyzed range. Finally, the belt elasticity has a very low effect on both the transmission capability and energy efficiency of the system: some appreciable effects arise for very low value of belt stiffness which causes a reduction of the transmission capability and an increase of the dissipated energy.

For each simulation the dissipated energy has been divided in energy dissipated due to sliding friction and energy dissipated due to non-recoverable elastic deformation of the belt, on both the driving and the driven pulley. The results showed that, for non-negligible values of transmitted torque, the higher source of energy dissipation is friction along the driving pulley.

These results are very important in the simulation of transmission (e.g. real-time systems, hardware in the loop systems) since they allow to introduce the phenomenological behavior of the pulley-belt transmission without introducing complex and computationally heavy models in the simulation. An experimental campaign has been planned to experimentally validate the model.

References

[1] Kong L and Parker R G 2005 Microslip friction in flat belt drives *Proceedings of the Institution of Mechanical Engineers, Part C: Journal of Mechanical Engineering Science* **10** 1097–1106

[2] Frendo F and Bucchi F 2020 ”Brush model” for the analysis of flat belt transmissions in steady-state conditions*Mechanism and Machine Theory* **143** 103653

[3] Bernard J E, Segel L and Wild R E 1977 Tire shear force generation during combined steering and braking maneuvers *SAE Technical Paper* 770852

[4] Bertini L, Carmignani L and Frendo F 2014 Analytical model for the power losses in rubber V-belt continuously variable transmission (CVT) *Mechanism and Machine Theory* **78** 289–306

[5] Pacejka H B and Sharp R S 1991 Shear force development by pneumatic tyres in steady state conditions: a review of modelling aspects *Vehicle System Dynamics* **3–4** 121–175

[6] Della Pietra L and Timpone F 2013 Tension in a flat belt transmission: experimental investigation *Mechanism and Machine Theory* **70** 129–156

[7] Kim H, Marshek K and Naji M 1987 Forces between an abrasive belt and pulley *Mechanism and Machine Theory* **1** 97–103

[8] Schallamach A 1971 How does rubber slide? *Wear* **17** 301–312

[9] Fukahori Y, Gabriel P and Busfiled J J C 2010 How does rubber truly slide between Schallamach waves and stick–slip motion? *Wear* **269** 854–866

[10] Frendo F and Bucchi F 2020 Enhanced brush model for the mechanics of power transmission in flat belt drives under steady–state conditions: Effect of belt elasticity *Mechanism and Machine Theory* **153** 103998